Drug Development Series: Review

How molecular imaging is speeding up antiangiogenic drug development

Weibo Cai,[1] Jianghong Rao,[1] Sanjiv S. Gambhir,[1,2] and Xiaoyuan Chen[1]

[1]The Molecular Imaging Program at Stanford, Department of Radiology and Bio-X Program and [2]Department of Bioengineering, Stanford University School of Medicine, Stanford, California

Abstract

Drug development is a long process that generally spans about 10 to 15 years. The shift in recent drug discovery to novel agents against specific molecular targets highlights the need for more robust molecular imaging platforms. Using molecular probes, molecular imaging can aid in many steps of the drug development process, such as providing whole body readout in an intact system, decreasing the workload and speeding up drug development/validation, and facilitating individualized anticancer treatment monitoring and dose optimization. The main focus of this review is the recent advances in tumor angiogenesis imaging, and the targets include vascular endothelial growth factor and vascular endothelial growth factor receptor, integrin $\alpha_v\beta_3$, matrix metalloproteinase, endoglin (CD105), and E-selectin. Through tumor angiogenesis imaging, it is expected that a robust platform for understanding the mechanisms of tumor angiogenesis and evaluating the efficacy of novel antiangiogenic therapies will be developed, which can help antiangiogenic drug development in both the preclinical stage and the clinical settings. Molecular imaging has enormous potential in improving the efficiency of the drug development process, including the specific area of antiangiogenic drugs. [Mol Cancer Ther 2006;5(11):2624–33]

Received 7/10/06; revised 8/29/06; accepted 9/12/06.

Grant support: National Institute of Biomedical Imaging and Bioengineering grant R21 EB001785; National Cancer Institute grants R21 CA102123, P50 CA114747, U54 CA119367, and R24 CA93862; Department of Defense grant W81XWH-04-1-0697, W81XWH-06-1-0665, W81XWH-06-1-0042, and DAMD17-03-1-0143; and Benedict Cassen Postdoctoral Fellowship from the Education and Research Foundation of the Society of Nuclear Medicine (W. Cai).

Requests for reprints: Xiaoyuan Chen, The Molecular Imaging Program at Stanford, Department of Radiology and Bio-X Program, Stanford University School of Medicine, 1201 Welch Road, P095, Stanford, CA 94305-5484. Phone: 650-725-0950; Fax: 650-736-7925. E-mail: shawchen@stanford.edu

doi:10.1158/1535-7163.MCT-06-0395

Introduction

Cancer drug discovery is a relatively long process. Rational predefined steps have been streamlined for drug development in recent years, thanks to the development of many new technologies (Fig. 1). Many imaging techniques have been routinely used in the drug discovery process to directly monitor the drug in blood, normal, and tumor tissues and to evaluate the effects of the drug in the context of tumor (1, 2). Anatomic/functional imaging modalities, such as computed tomography, magnetic resonance imaging, and ultrasound, have been used to assess tumor size and structure. They can also provide valuable information on tumor perfusion, integrity of the blood-brain barrier, vessel density, vessel permeability, blood oxygenation, blood volume, blood flow, blood velocity, and flow resistance. However, with the recent shift in drug discovery from conventional cytotoxic drugs to novel agents against specific molecular targets, these conventional imaging modalities are usually no longer adequate. Cytostatic therapies are much less toxic, and disease stabilization may not lead to shrinkage of tumors in a short period of time. Molecular imaging recently emerges with increasing popularity as it can be used to monitor the changes at the molecular level *in vivo*, and it can help in evaluating treatment efficacy much earlier.

Molecular imaging refers to the characterization and measurement of biological processes at the molecular level (3). For a representative comprehensive review, the readers are referred to ref. 3. Molecular imaging techniques include positron emission tomography (PET), single-photon emission computed tomography (SPECT), molecular magnetic resonance imaging, magnetic resonance spectroscopy, optical bioluminescence, optical fluorescence, and targeted ultrasound (3). Molecular imaging can give whole body readout in an intact system, help to decrease the workload and speed up the drug development process, provide more statistically relevant results because longitudinal studies can be done in the same animals, aid in lesion detection and patient stratification, and help in individualized anticancer treatment monitoring and dose optimization.

Several excellent review articles have been published on the general role of molecular imaging on drug development (2, 4–6). For the remaining of this review article, we will mainly focus on expounding the role of molecular imaging in antiangiogenic drug development and briefly summarize the recent advances in tumor angiogenesis imaging.

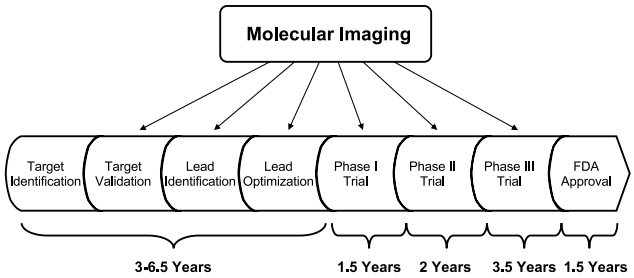

Figure 1. Drug development is a relatively long process, which usually spans 10 to 15 years. Molecular imaging can help in many steps of the process.

Tumor Angiogenesis

Angiogenesis, the formation of new blood vessels from preexisting blood vessels, is a fundamental process occurring during tumor progression (7). Tumor growth depends on the balance between proangiogenic and antiangiogenic molecules. Molecules regulating angiogenesis include, but are not limited to, growth factor receptors, tyrosine kinase receptors, G-protein–coupled receptors for angiogenesis modulating proteins, integrins, and matrix metalloproteinases (MMP; ref. 8). Here, we will focus on three of the most intensively studied angiogenesis-related molecular targets: vascular endothelial growth factor (VEGF) and VEGF receptors (VEGFR), integrin $\alpha_v\beta_3$, and MMPs (Fig. 2). During tumor angiogenesis, these molecules interact closely with each other. Integrin $\alpha_v\beta_3$ can recruit and activate MMP-2, which degrades components of the basement membrane and interstitial matrix to facilitate tumor progression (9). It can also regulate the production of VEGF in certain tumor cells (10). Several other molecular targets that are also involved in tumor angiogenesis are thus far understudied and will only be briefly mentioned, such as endoglin (CD105) and E-selectin (Fig. 2).

Imaging VEGF and VEGFR Expression

VEGF is a potent mitogen in embryonic and somatic angiogenesis. It plays a central role in both normal vascular tissue development and tumor neovascularization (8). The VEGF family is comprised of seven members with a common VEGF homology domain: VEGF-A, VEGF-B, VEGF-C, VEGF-D, VEGF-E, VEGF-F, and placental growth factor. VEGF-A is a dimeric, disulfide-bound glycoprotein that exists in at least seven homodimeric isoforms, consisting of 121, 145, 148, 165, 183, 189, or 206 amino acids (11). These isoforms differ not only in their molecular weight but also in biological properties, such as the ability to bind to cell surface heparin sulfate proteoglycans.

The angiogenic actions of VEGF are mainly mediated via two closely related endothelium-specific receptor tyrosine kinases: Flt-1 (VEGFR-1) and Flk-1/KDR (VEGFR-2; ref. 12). Both are largely restricted to vascular endothelial cells and are overexpressed on the endothelium of tumor vasculature, whereas they are almost undetectable in the vascular endothelium of adjacent normal tissues. All of the VEGF-A isoforms bind to both VEGFR-1 and VEGFR-2. It is generally agreed that VEGFR-1 is critical for physiologic and developmental angiogenesis, and the function of VEGFR-1 differs with the stages of development, the states of physiologic and pathologic conditions, and the cell types in which it is expressed (12). VEGFR-2 is the major mediator of the mitogenic, angiogenic, and permeability-enhancing effects of VEGF. Overexpression of VEGFR or VEGF-A has been implicated as poor prognostic markers in various clinical studies of cancer (13). Agents that prevent VEGF-A binding to its receptors, antibodies that directly block VEGFR-2, and small molecules that inhibit the kinase activity of VEGFR-2 thereby blocking VEGF/VEGFR signaling are all under active development (14–16). The critical role of VEGF-A in cancer progression has been highlighted by the recent approval of the humanized anti-VEGF monoclonal antibody bevacizumab (Avastin; Genentech, South San Francisco, CA) for first-line treatment (17). Successful development of VEGF- or VEGFR-targeted molecular imaging could serve as a paradigm for the assessment of cancer therapeutics targeting tumor angiogenesis.

Recombinant human $VEGF_{121}$ has been labeled with ^{111}In for identification of ischemic tissue in a rabbit model, where unilateral hind limb ischemia was created by femoral artery excision (18). However, virtually no difference was observed between the ischemic hind limb and the contralateral hind limb. $VEGF_{121}$ has also been labeled with ^{99m}Tc through an ''Adapter/Docking'' strategy (19). The tracer was used to image 4T1 murine mammary carcinoma, and very low tumor signal (<3 %ID/g) was observed. Recently, this tracer was also tested for the imaging of tumor vasculature before and after different types of chemotherapy (20). $[^{123}I]VEGF_{165}$ has also been reported as a potential tumor marker (21). Despite the high receptor affinity of this tracer, biodistribution in A2508 melanoma tumor-bearing mice indicated poor tumor-to-background ratio, most likely due to the low metabolic stability of the compound. Nonetheless, biodistribution, safety, and absorbed dose of $[^{123}I]VEGF_{165}$ was studied in patients with pancreatic carcinoma (22). Following i.v. administration, sequential images were

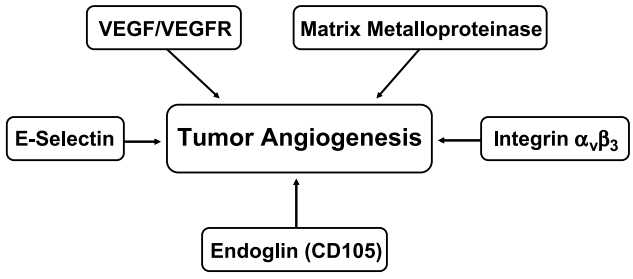

Figure 2. Representative molecular targets involved in tumor angiogenesis.

recorded during the initial 30 minutes after injection. Although a majority of primary pancreatic tumors and their metastases were visualized by [^{123}I]VEGF$_{165}$ scan, the organ with the highest absorbed doses was the thyroid, indicating severe deiodination of the probe. A recombinant protein composed of VEGF$_{165}$ fused through a flexible polypeptide linker $(GGGGS)_3$ to the n-lobe of human transferrin was also reported for imaging angiogenesis, and the tumor contrast was modest (23). In all the above reports, radiolabeled VEGF isoforms were used for SPECT imaging. PET has several advantages over SPECT, including 1 to 2 orders of magnitude greater sensitivity, and the increasing implementation of clinical PET and PET/CT (computed tomography) scanners can facilitate the translation of novel PET tracers to the clinic.

A few radiolabeled anti-VEGF antibodies have been reported for PET imaging applications. VG76e, an IgG1 monoclonal antibody that binds to human VEGF, was labeled with ^{124}I for PET imaging of solid tumor xenografts in immunodeficient mice (24). Whole-animal PET imaging studies revealed a high tumor-to-background contrast (Fig. 3A). Although VEGF specificity *in vivo* was shown in this report, the poor immunoreactivity (<35%) of the radiolabeled antibody limits the potential use of this tracer. HuMV833, a humanized version of a mouse monoclonal anti-VEGF antibody MV833, was also labeled with ^{124}I, and the distribution and biological effects of HuMV833 in phase I trial cancer patients were investigated (25). Patients with progressive solid tumors were treated with various doses of HuMV833, and PET imaging using [^{124}I]HuMV833 was carried out to measure the antibody distribution. It was found that antibody distribution and clearance were quite heterogeneous not only between patients but also between individual tumors of the same patient, suggesting that intra-patient dose escalation approaches or more precisely defined patient cohorts would be preferred in the design of phase I studies with antiangiogenic antibodies such as HuMV833.

We have recently labeled VEGF$_{121}$ with ^{64}Cu ($t_{1/2}$ = 12.7 hours) for PET imaging of tumor angiogenesis and VEGFR expression (26). DOTA-VEGF$_{121}$ (where DOTA denotes 1,4,7,10-tetraazacyclododecane-1,4,7,10-tetraacetic acid) exhibits nanomolar receptor binding affinity *in vitro*. MicroPET imaging revealed rapid, specific, and prominent uptake of [^{64}Cu]DOTA-VEGF$_{121}$ in highly vascularized small U87MG tumor (high VEGFR-2 expression) but significantly lower and sporadic uptake in large U87MG tumor (low VEGFR-2 expression; Fig. 3B). Western blot of tumor tissue lysate, immunofluorescence staining, and blocking studies with unlabeled VEGF$_{121}$ confirmed that the *in vivo* tumor uptake is VEGFR specific. Substantial tracer uptake in the kidneys was also observed, most likely due to the high VEGFR-1 expression in this organ. Successful demonstration of the ability of [^{64}Cu]DOTA-VEGF$_{121}$ to visualize VEGFR expression *in vivo* should allow for clinical translation of this tracer to image tumor angiogenesis and to guide antiangiogenic treatment, especially VEGFR-targeted cancer therapy. Based on the *in vivo* pharmacokinetics of [^{64}Cu]DOTA-VEGF$_{121}$, VEGF$_{121}$ may also be labeled with ^{18}F for PET imaging applications as good tumor-to-background ratio was achieved as early as 1 to 2 hours after injection.

The abovementioned examples showed that molecular imaging of tumor angiogenesis can play a role in target validation, lead optimization, monitoring therapeutic response, and in clinical trials during the drug development process. Despite the critical role of VEGF and VEGFR in tumor angiogenesis, molecular imaging of VEGF or VEGFR has not been well studied. In the clinical setting, the right timing can be critical for VEGFR-targeted cancer therapy, and PET imaging of VEGF/VEGFR can play a very important role in determining whether to start and when to start the VEGFR-targeted treatment. Clinical translation will be critical for the maximum benefit of VEGF-based cancer imaging agents. Much research remains to be done in the near future to optimize VEGF- or VEGFR-targeted

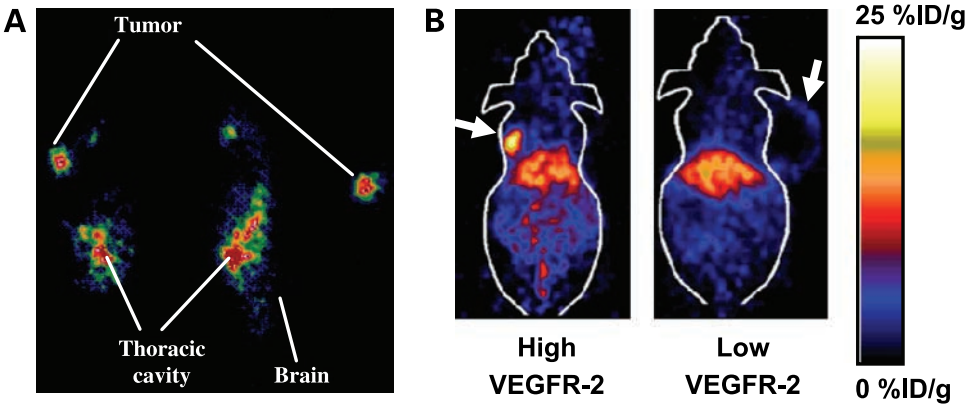

Figure 3. **A,** PET images of a tumor-bearing mouse at 24 h after injection of ^{124}I-labeled VG76e. *Left* to *right,* coronal, sagittal, and transverse views. **B,** microPET images of U87MG tumor-bearing mice 16 h after injection of [^{64}Cu]DOTA-VEGF$_{121}$. The small tumor has high VEGFR-2 expression, whereas the large tumor has low VEGFR-2 expression. %ID/g, percent injected dose per gram of tissue (adapted from refs. 24, 26).

molecular imaging. Site-specific labeling via a Cys-tag may offer advantage over direct labeling on the amino group of the lysine side chain for new tracer development or tracer optimization. A VEGFR-2-specific ligand can also be developed, which may be superior to VEGF-A-based tracer, as experimental evidence has shown that VEGFR-2 is more involved in tumor angiogenesis, whereas VEGF-A binds to both VEGFR-1 and VEGFR-2. Peptidic VEGFR antagonists, which can be labeled with ^{11}C or ^{18}F (more readily available than ^{64}Cu or ^{124}I), may also be tested (27). Peptide-based tracers may allow for higher throughput than antibody- or protein-based radiotracers, as 1-hour after injection is usually sufficient for a peptide-based tracer to clear from the non-targeted organs and give high-contrast PET images. In contrast, it may take several hours and even days before high-contrast PET images can be obtained for protein- or antibody-based tracer. Transgenic mouse models where either the VEGF or VEGFR-2 promoter drives reporter gene expression will also likely play a useful role in understanding VEGF biology and drug optimization (28).

As VEGF/VEGFR signaling is one of the most important pathways during tumor angiogenesis, the ability to image and quantify VEGF and/or VEGFR expression level during tumor growth and upon antiangiogenic treatment will be of critical importance. It has been shown that the therapeutic window of VEGF/VEGFR–targeted delivery does not depend on the total dose given but rather on the microenvironmental levels of VEGF/VEGFR expression. Visualizing and quantifying VEGF/VEGFR expression *in vivo* will allow for personalized treatment by choosing the right timing during which the treatment is most effective. *In vivo* imaging of VEGF/VEGFR expression will also be able to determine the effective dose of VEGF/VEGFR–based treatment, so that therapeutically efficacious dose levels can be given safely.

Imaging Integrin $\alpha_v\beta_3$ Expression

Integrins are a family of cell adhesion molecules consisting of two noncovalently bound transmembrane subunits (α and β), both type I membrane proteins with large extracellular segments that pair to create heterodimers with distinct adhesive capabilities (29). In mammals, 18 α and 8 β subunits assemble into 24 different receptors. Integrin signaling plays a key role in tumor angiogenesis and metastasis (30). Integrins expressed on endothelial cells modulate cell migration and survival during angiogenesis, whereas integrins expressed on carcinoma cells potentiate metastasis by facilitating invasion and movement across blood vessels. The $\alpha_v\beta_3$ integrin, which binds to arginine-glycine-aspartic acid (RGD)–containing components of the interstitial matrix, is significantly up-regulated on endothelium during angiogenesis but not on quiescent endothelium (30, 31). Inhibition of $\alpha_v\beta_3$ integrin activity by monoclonal antibodies, cyclic RGD peptide antagonists, and peptidomimetics has been shown to induce endothelial cell apoptosis, to inhibit angiogenesis, and to increase endothelial monolayer permeability (32).

Crystal structure of the extracellular portion of integrin $\alpha_v\beta_3$ in complex with c(RGDf(NMe)V) has been reported (31, 33). The cyclic RGD peptide binds at the major interface between the α_v and β_3 subunits and makes extensive contacts with both in a transition metal (e.g., Mn^{2+})–dependent mode. Preclinical studies indicated that many integrins other than $\alpha_v\beta_3$ also play important roles in regulating angiogenesis, such as $\alpha_1\beta_1$, $\alpha_2\beta_1$, $\alpha_4\beta_1$, $\alpha_5\beta_1$, $\alpha_6\beta_4$, $\alpha_{IIb}\beta_3$, and $\alpha_v\beta_5$ (32). Among all 24 integrins discovered to date, integrin $\alpha_v\beta_3$ is the most intensively studied, and an extensive review on multimodality molecular imaging of integrin $\alpha_v\beta_3$ has recently been published (34).

Non–Radionuclide-Based Imaging of Integrin $\alpha_v\beta_3$ Expression

Antibody-coated paramagnetic liposomes (35), Gd-perfluorocarbon nanoparticles conjugated to anti-integrin $\alpha_v\beta_3$ monoclonal antibody (36), and integrin $\alpha_v\beta_3$-targeted paramagnetic nanoparticles (37) have been reported for magnetic resonance imaging of integrin $\alpha_v\beta_3$ expression (Fig. 4A). In these studies, the targeted paramagnetic nanoparticles are coated with either antibodies or small peptidic/peptidomimetic integrin $\alpha_v\beta_3$ antagonists. Because of the relatively large size of the probes (200–700 nm), these agents target the integrin $\alpha_v\beta_3$ expressed on the tumor vasculature rather than the tumor cells. Ultrasound imaging using integrin $\alpha_v\beta_3$–targeted microbubbles has also been reported (Fig. 4B; ref. 38). Because acoustic destruction of ''payload-bearing'' microbubbles can be used to deliver drugs or to augment gene transfection (39), integrin $\alpha_v\beta_3$–targeted microbubbles may have applications in site-specific cancer therapy. Further studies are needed to validate the potential therapeutic applications.

Although optical imaging may not be widely used in clinical settings, near-IR (700–900 nm) approaches provide opportunities for rapid and cost-effective preclinical evaluation in small animal models before the more costly radionuclide-based imaging studies. These approaches may also be translated into the clinic with fluorescence-mediated tomography (e.g., for breast cancer imaging). In the near-IR region, the absorbance of all biomolecules reaches minima, providing a clear window for *in vivo* optical imaging (40). We have shown that near-IR fluorescent dye or quantum dot–conjugated cyclic RGD peptide could be used to visualize s.c. inoculated integrin $\alpha_v\beta_3$–positive tumors (41, 42). The dye-RGD peptide conjugate is small in size; therefore, it targets integrin $\alpha_v\beta_3$ on both tumor cells and tumor vasculature (Fig. 4C). For the quantum dot-RGD peptide conjugate, it mainly targets integrin $\alpha_v\beta_3$ in the tumor vasculature because it does not extravasate well due to the relatively large size ($\geq$20 nm; Fig. 4D). Based on these results, an approach that takes advantage of the high integrin $\alpha_v\beta_3$–targeting efficacy of the cyclic RGD peptides, high stability and brightness of quantum dots, and emission wavelength in the near-IR window will have great potential

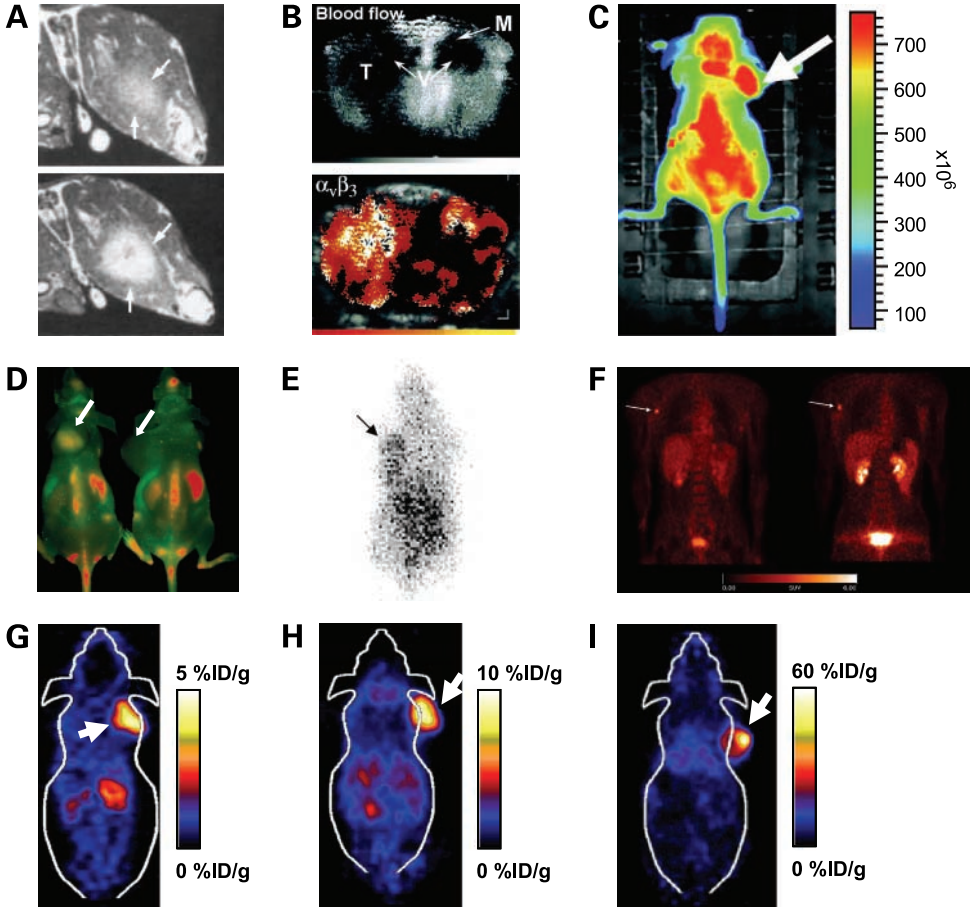

Figure 4. **A,** magnetic resonance images of an i.m. tumor before (*top*) and after (*bottom*) administration of integrin $\alpha_v\beta_3$–targeted liposomes. **B,** contrast-enhanced ultrasound images of a tumor-bearing rat depicting parametric perfusion data (*top*) and signal enhancement from integrin $\alpha_v\beta_3$–targeted microbubbles (*bottom*). *T,* tumor; *V,* ventricles; *M,* a periventricular metastasis. **C,** *in vivo* near-IR fluorescence imaging of s.c. U87MG tumor-bearing mice 1 h after administration of RGD-Cy5.5 conjugate. **D,** *in vivo* near-IR fluorescence imaging of U87MG tumor-bearing mice injected with quantum dot-RGD conjugate (*left*) or equal amount of unconjugated quantum dot (*right*). **E,** scintigraphic image of an ovarian carcinoma tumor-bearing mouse 2 h after administration of an ^{111}In-labeled dimeric RGD peptide. **F,** a patient with malignant melanoma stage IIIb and a solitary lymph node metastasis in the right axilla was visualized by both [^{18}F]FDG (*left*) and [^{18}F]galacto-RGD (*right*). **G,** coronal microPET image of a U87MG tumor-bearing mouse 70 min after administration of [^{18}F]FRGD2. **H,** coronal microPET image of a U87MG tumor-bearing mouse 1 h after administration of [^{64}Cu]DOTA-E[E[c(RGDfK)]$_2$]$_2$. **I,** coronal microPET image of a U87MG tumor-bearing mouse 25 h after administration of [^{64}Cu]DOTA-Abegrin. The tumors are shown with arrows in all cases (adapted from refs. 35, 38, 41, 42, 45, 50, 55, 60, 61).

in cancer diagnosis and imaging as well as imaging-guided surgery and therapy.

Recently, Achilefu et al. (43) discovered that conjugating a presumably inactive linear hexapeptide GRDSPK with an near-IR carbocyanine molecular probe yielded Cyp-GRD that targets integrin $\alpha_v\beta_3$–positive tumors. More experiments need to be carried out to fully understand this surprising phenomenon, and docking study may reveal whether Cyp-RGD actually binds to the RGD binding domain in integrin $\alpha_v\beta_3$. Later, they synthesized and evaluated a series of multimeric RGD compounds constructed on a dicarboxylic acid–containing near-IR fluorescent dye cypate for tumor targeting (44). Optimization of the spatial alignment of the RGD moieties through careful molecular design and library construction may induce multivalent ligand-receptor interactions useful for *in vivo* tumor imaging and tumor-targeted therapy.

SPECT/PET Imaging of Integrin $\alpha_v\beta_3$ Expression

RGD peptides have been labeled with ^{111}In and ^{99m}Tc for SPECT imaging of integrin $\alpha_v\beta_3$ expression. The *in vivo* behavior of radiolabeled dimeric RGD peptide E[c(RGDfK)]$_2$ was studied in an ovarian carcinoma xenograft model (45). ^{111}In/^{90}Y and ^{99m}Tc were incorporated through DOTA and hydrazinonicotinamide (HYNIC) chelators, respectively (Fig. 4E). RP748, an ^{111}In-labeled quinolone that binds to integrin $\alpha_v\beta_3$ with high affinity, was recently studied both *in vitro* and *in vivo* to track injury-induced vascular proliferation in rodents (46). Water-soluble *N*-(2-hydroxypropyl)methacrylamide copolymers have

been synthesized with pending doubly cyclized RGD peptides (47). The bioactivity of the polymer conjugates and free peptides was characterized both *in vitro* and *in vivo*. It was shown that specific targeting of $\alpha_v\beta_3$ integrin and nonspecific vascular permeability both contributed significantly to the tumor uptake, with specific targeting being more important. It was concluded that peptide oligomers may be more suitable for imaging purposes because of the rapid clearance, whereas peptide-polymer conjugates may be used for high-level targeting and radiotherapeutic approaches.

PET has been the mainstay of integrin $\alpha_v\beta_3$ expression imaging, and most reports focus on the radiolabeling of RGD peptide antagonists. Monomeric RGD peptide c(RGDyV) was first labeled with ^{125}I by Haubner et al. (48). A glycopeptide based on c(RGDfK) was later labeled with ^{18}F via a 2-[^{18}F]fluoropropionate prosthetic group, and the resulting [^{18}F]galacto-RGD exhibited integrin $\alpha_v\beta_3$–specific tumor uptake in integrin-positive M21 melanoma xenograft model (49). Initial clinical trials in healthy volunteers and a limited number of cancer patients revealed that this tracer can be safely given to patients and is able to delineate certain lesions that are integrin positive (Fig. 4F; ref. 50). Despite the successful translation of [^{18}F]galacto-RGD into clinical trials, several key issues remain to be resolved, such as tumor-targeting efficacy, pharmacokinetics, and the ability to quantify integrin $\alpha_v\beta_3$ density *in vivo*.

We have labeled a series of RGD peptides with ^{18}F for PET imaging, using PEGylation and polyvalency to improve the tumor-targeting efficacy and pharmacokinetics (51–56). [^{18}F]FB-E[c(RGDyK)]$_2$ (abbreviated as [^{18}F]FRGD2) had predominant renal excretion and almost twice as much tumor uptake in the same animal model compared with the monomeric tracer [^{18}F]FB-c(RGDyK) (Fig. 4G; refs. 54, 55). The synergistic effect of polyvalency and improved pharmacokinetics may be responsible for the excellent imaging characteristics of [^{18}F]FRGD2. Graphical analyses of the dynamic microPET scans in six tumor xenograft models were carried out to correlate the tumor uptake with integrin $\alpha_v\beta_3$ expression level measured by SDS-PAGE autoradiography, and excellent linear correlation was observed. More importantly, it was found that at late time points when most of the nonspecific binding had been cleared, the tumor/background ratio had a linear relationship with tumor integrin $\alpha_v\beta_3$ expression level, thus making it possible to quantify integrin $\alpha_v\beta_3$ density *in vivo*. We are currently in the process of translating [^{18}F]FRGD2 into the clinic for cancer patient imaging.

In addition to ^{18}F, ^{64}Cu-labeled RGD peptides are also of considerable interest. Copper-64 is an attractive radionuclide for both PET imaging and targeted radiotherapy of cancer. PET imaging of tumors with low doses of ^{64}Cu-labeled RGD peptides may be used to determine radiation dosimetry before therapy with high dose of ^{64}Cu- or ^{67}Cu-labeled RGD peptides. We have labeled RGD peptides with ^{64}Cu for PET imaging, again using PEGylation and polyvalency to optimize the tumor-targeting efficacy and pharmacokinetics (53, 57–59). Recently, we reported a tetrameric RGD peptide-based tracer, [^{64}Cu]DOTA-E[E[c(RGDfK)]$_2$]$_2$, which showed significantly higher receptor binding affinity than the corresponding monomeric and dimeric RGD analogues (60). This tracer exhibited rapid blood clearance, high metabolic stability, predominant renal excretion, significant receptor-mediated tumor uptake, and good contrast in xenograft-bearing mice (Fig. 4H). The high integrin avidity and favorable biokinetics makes [^{64}Cu]DOTA-E[E[c(RGDfK)]$_2$]$_2$ a promising agent for peptide receptor radionuclide imaging as well as targeted internal radiotherapy of integrin $\alpha_v\beta_3$–positive tumors.

Abegrin (MEDI-522, also called Vitaxin; MedImmune, Inc., Gaithersburg, MD), a humanized monoclonal antibody against human integrin $\alpha_v\beta_3$ (picomolar binding affinity), is in clinical trials for cancer therapy. We have conjugated Abegrin with macrocyclic chelating agent DOTA and labeled it with ^{64}Cu for PET imaging of tumor xenografts (61). MicroPET studies revealed that [^{64}Cu]DOTA-Abegrin had very high tumor uptake in integrin $\alpha_v\beta_3$–positive U87MG tumor (Fig. 4I). The receptor specificity of [^{64}Cu]DOTA-Abegrin was confirmed by effective blocking of tumor uptake with coadministration of nonradioactive Abegrin. The success of integrin $\alpha_v\beta_3$–specific tumor imaging using [^{64}Cu]DOTA-Abegrin may be translated into the clinic to characterize the pharmacokinetics, tumor-targeting efficacy, dose optimization, and dose interval of Abegrin and/or Abegrin conjugates. Chemotherapeutics or radiotherapeutics using Abegrin as the delivering vehicle may also be effective in treating integrin $\alpha_v\beta_3$–positive tumors.

Integrin $\alpha_v\beta_3$ is one of the most extensively studied molecular targets involved in tumor angiogenesis (30–34). The numerous reports on multimodality molecular imaging of integrin $\alpha_v\beta_3$ again showed that tumor angiogenesis imaging can participate in multiple stages of the drug development process, such as target validation, lead optimization, and clinical trials. However, to date, only [^{18}F]galacto-RGD has advanced into clinical settings for further testing, and the tracer itself is probably suboptimal (62). Polyvalent integrin $\alpha_v\beta_3$ antagonists, such as multimeric RGD peptides, are also promising ligands for the molecular targeting of integrins involved in tumor angiogenesis. Translation of new multimeric RGD peptide-based tracers into the clinic will dramatically benefit antiangiogenic cancer therapy based on integrin $\alpha_v\beta_3$ antagonism. The ability to quantify integrin $\alpha_v\beta_3$ expression level *in vivo* will be very important in monitoring antiangiogenic treatment efficacy. Some of the abovementioned tracers with high integrin $\alpha_v\beta_3$-positive tumor uptake, as shown by molecular imaging studies, may also have the potential to evolve into radioimmunotherapeutic agents for cancer therapy.

Imaging MMP Expression

MMPs are a family of Zn^{2+}-dependent endopeptidases, which play important roles in tumor angiogenesis, in

particular the 72-kDa (MMP-2) and 92-kDa (MMP-9) gelatinases (63). MMP-2, capable of degrading type IV collagen (major component of the basement membranes), can be localized in a proteolytically active form on the surface of invasive cancer cells based on its ability to bind to integrin $\alpha_v\beta_3$ (9). A number of MMP inhibitors (MMPI) have been developed as cytostatic and antiangiogenic agents and are currently in clinical testing (64). Until recently, clinical trials with MMPIs have yielded disappointing results, highlighting the need for better insight into the mechanisms by which MMPs contribute to tumor growth. Molecular imaging to monitor MMP expression noninvasively *in vivo* will be critical for future drug development targeting MMPs.

Molecular imaging of MMP expression, as well as imaging of other enzymes, can be divided into two approaches. In the ''targeted'' probes approach, labeled small molecules, peptides, metabolites, aptamers, antibodies, or other molecules are injected i.v., and the living systems can be imaged when a fraction of the agent has bound to its target and the non-bound agent has been cleared. Non-peptidyl broad-spectrum MMPIs, tissue inhibitors of metalloproteinases, MMP-2-specific inhibitors, carboxylic and hydroxamic acid–based MMPIs, selective inhibitors of MMP-2/MMP-9, and other MMPIs have been labeled with ^{123}I, ^{125}I, ^{111}In, ^{99m}Tc, ^{11}C, ^{18}F, and/or ^{64}Cu for *in vivo* biological and clinical investigation of MMP expression using SPECT and PET (65–72). However, in most of the reports, selective binding of the labeled compounds to specific MMPs was not shown, and high nonspecific binding was observed possibly due to low *in vivo* stability of the tracers. Except for one most recent report (Fig. 5A; ref. 71), none of the abovementioned reports showed any convincing *in vivo* imaging results. The cyclic decapeptide CTTHWGFTLC, a selective MMP-2 and MMP-9 inhibitor, was conjugated with DOTA and labeled with ^{64}Cu for PET imaging of MMP expression in xenograft models. Zymography of tumor extracts supported the *in vivo* PET imaging results. MMP-2 and MMP-9 bands were clearly detectable in the mouse imaged at 7 weeks, which had prominent tumor uptake, whereas the MMP-2 and MMP-9 expression was very week afterwards, which gave low tumor uptake (Fig. 5A). However, MMP expression in the MDA-MB-435 tumor model used in this study had quite large individual variance. The low *in vivo* stability of the radiotracer also limits further application of this strategy.

The abovementioned approach based on affinity ligands is usually more useful for imaging receptors and cell surface–expressed molecules, but it may not be the best approach for imaging enzyme function in a living organism. Another approach is the use of ''activatable probes.'' Activatable probes undergo chemical or physicochemical changes on target interaction and result in signal amplification. This approach was first shown by Bremer et al. where MMP activity was imaged in live animals, and that the inhibition of MMP activity can be recorded within hours after treatment by a potent MMPI (Fig. 5B; refs. 73, 74). Later, similar approaches were used for imaging MMP expression in the heart after myocardial

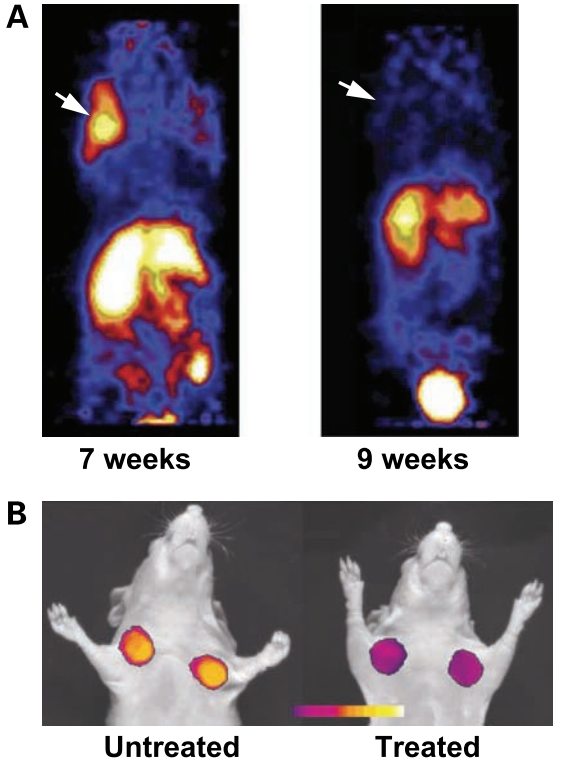

Figure 5. **A,** microPET imaging of a ^{64}Cu-labeled MMP-2/MMP-9 inhibitor in MDA-MB-435 breast tumor-bearing mice at 7 wks (*left*, where MMP-2/MMP-9 expression is clearly detectable by zymography) and 9 wks (*right*, where MMP-2/MMP-9 expression is not detectable by zymography) after inoculation. **B,** *in vivo* near-IR fluorescence imaging of tumor-bearing mice using an activatable probe before (*left*) and after (*right*) prinomastat (a MMPI) treatment (adapted from refs. 71, 74).

infarction where an near-IR fluorescent probe was activated upon proteolytic cleavage by MMP-2 and MMP-9 (75). In another report, cellular association of polyarginine-based cell-penetrating peptides is effectively blocked when they are fused to an inhibitory domain composed of negatively charged residues, which was called ''activatable cell-penetrating peptides'' (76). Cleavage of the MMP-sensitive linker between the polycationic and polyanionic domains releases the cell-penetrating peptide portion and its attached cargo to bind to and enter cells. In xenograft tumor models expressing MMP-2/MMP-9, a fluorescent dye Cy5-conjugated activatable cell-penetrating peptide showed modest *in vivo* tumor contrast (2- to 3-fold when compared with contralateral normal tissue). The similar approach has also been applied to modulate the cellular uptake of quantum dot conjugates (77). Another fluorogenic activatable probe, which is MMP-7 selective, has been reported for *in vivo* detection and imaging of tumor-associated MMP-7 activity (78). Although the activatable probe strategy may give good tumor/background contrast, the major drawback of optical imaging is that it has limited clinical applications.

In vivo imaging of MMP expression is still underdeveloped due to many issues. First, the expression level of

MMPs varies during different stages of tumor progression, and imaging may also be complicated by naturally occurring tissue inhibitors of metalloproteinases. Second, specificity for one particular MMP is hard to achieve. There is still plenty of room for improving the selectivity between different MMPs, especially MMP-2 and MMP-9. The experimental outcome would be much better interpreted if the ligand is specific for one particular MMP. Third, quantifying the MMP expression level *in vivo* has not been demonstrated. The imaging results reported thus far are mostly qualitative. The ability of correlating the MMP imaging result with the MMP expression *in vivo* will dramatically help the advancement of MMP imaging, anti-MMP drug screening, and monitoring of treatment efficacy.

Imaging Endoglin and E-Selectin

In vivo imaging of endothelial markers in intact tumor neovasculature can significantly help assessing the efficacy of antiangiogenic agents in clinical trials. Although many endothelial markers have been described, only few of them have been evaluated as imaging markers. Endoglin (CD105) is emerging as a prime vascular target for anti-angiogenic cancer therapy (79). It is a cell membrane glycoprotein mainly expressed on endothelial cells and overexpressed on tumor vasculature. It functions as an accessory component of the transforming growth factor-β receptor complex and is involved in vascular development and remodeling. Avidin-coated microbubbles have been linked to biotinylated monoclonal antibodies for endoglin targeting *in vitro* (80). ^{125}I-labeled monoclonal antibody MAEND3 has been reported to target CD105 on tumor vasculature in canine models (81). Another radiolabeled monoclonal anti-endoglin antibody has also been used for *in vivo* imaging (82). The major advantage of imaging abundantly expressed endothelial targets is that this strategy circumvents delivery barriers normally associated with other tumor-targeting strategies.

E-selectin is a cell adhesion molecule and CD antigen that mediates neutrophil, monocyte, and memory T-cell adhesion to cytokine-activated endothelial cells (83). It is expressed exclusively by activated endothelial cells, and it recognizes sialylated carbohydrate groups related to the Lewis X or Lewis A family. Fluorescence reflectance imaging (a photographic process that captures views of a surface under varying lighting conditions to enhance surface detail that may otherwise be difficult to see) of E-selectin expression in mouse xenograft models of Lewis lung carcinoma has been reported (84). The imaging probe was constructed by conjugating an E-selectin-binding peptide (CDSDSDITWDQLWDLMK) to CLIO(Cy5.5) nanoparticles, where CLIO represents cross-linked iron oxide that can be used for magnetic resonance imaging.

Endostatin, which binds fibulin and nidogen, is a 20-kDa COOH-terminal fragment of collagen XVIII, and it is a potent naturally occurring inhibitor of angiogenesis (7). It has been labeled with a fluorescent dye Cy5.5 for tumor localization after i.p. injection (85). Endostatin-Cy5.5 was quickly absorbed after administration, producing a near-IR fluorescence image of the tumors that persisted through 7 days. [^{99m}Tc]ethylenedicysteine-endostatin has also been synthesized for evaluating the efficacy of antiangiogenic therapy (86). Tissue distribution and planar imaging of radiolabeled endostatin were determined in tumor-bearing rats. It was claimed that [^{99m}Tc]ethylenedicysteine-endostatin could assess treatment response, and there was a correlation between tumor uptake and cellular targets expression level.

Conclusions and Perspectives

Significant advances have been made in developing novel probes for multimodality molecular imaging of tumor angiogenesis. Small molecules, peptides, peptidomimetics, proteins, and antibodies have been labeled with radioisotopes, superparamagnetic nanoparticles, fluorescent dyes, quantum dots, and microbubbles for PET, SPECT, magnetic resonance imaging, near-IR fluorescence, and ultrasound imaging of small animal tumor models, a few of which are now in early clinical trials. The major roles of tumor angiogenesis imaging in the drug development process will be the following: target identification, characterization, and validation; patient stratification (e.g., selecting the right population of cancer patients for new clinical trials); pharmacokinetic/pharmacodynamic studies (e.g., candidate drug screening and optimization, phase I clinical trials); as well as treatment monitoring and dose optimization (phase II/III trials). Through the development of a robust tumor angiogenesis imaging platform, molecular imaging can dramatically facilitate and speed up many steps of antiangiogenic drug development in both the preclinical and clinical stages.

Despite the strong potentials of angiogenesis imaging probes, most of the research efforts have thus far been limited to probe optimization for enhanced tumor-targeting efficacy and improved *in vivo* kinetics. The translation of the imaging probes from bench to bedside has been slow. The limited margins for marketing the very special probes makes some of *de novo* imaging approaches considered too risky by investigators. The situation is, however, being improved. Food and Drug Administration recently developed exploratory Investigational New Drug mechanism to allow faster first-in-human studies. Microdosing studies with novel imaging probes can provide an opportunity for early assessment of the safety profile and pharmacokinetics in healthy volunteers. Such rapid initial clinical studies will definitely accelerate the drug discovery process. Furthermore, the molecular imaging field has grown extremely fast over the last decade, and the value of molecular imaging in drug development and screening is more widely accepted by pharmaceutical companies. By repeated imaging in preclinical models using one or more of the discussed imaging strategies, one can have several readouts of angiogenesis before and after drug administration. Even if the drug target is different from the imaging target, one can still use imaging as a potential surrogate for the efficacy of the drug at a given dose. It is expected that in the foreseeable future molecular imaging will be routinely applied in many steps of the drug development process. The combination of

molecular and anatomic/functional imaging techniques in assessing tumor angiogenesis and in the response to antiangiogenic cancer therapy will be a powerful tool.

To foster the continued discovery and development of angiogenesis-targeted imaging probes, cooperative efforts are needed from cellular/molecular biologists to identify and validate molecular imaging targets, chemists/radiochemists to synthesize and characterize the imaging probes, and medical physicists/mathematicians to develop high-sensitivity/high-resolution imaging devices/hybrid instruments and to develop better algorithms to further improve signal-to-noise ratio of a given imaging device. Close partnerships among academic researchers, clinicians, pharmaceutical industries, the National Cancer Institute, and the Food and Drug Administration are also needed to promote further development of imaging probes, to apply molecular/functional imaging approaches to predict and evaluate antiangiogenic effect during and after treatment, to move molecular imaging guided intervention strategy quickly into the clinic, and to accelerate antiangiogenic drug development.

References

1. Gwyther SJ. New imaging techniques in cancer management. Ann Oncol 2005;16 Suppl 2:ii63 – 70.

2. Rudin M, Weissleder R. Molecular imaging in drug discovery and development. Nat Rev Drug Discov 2003;2:123 – 31.

3. Massoud TF, Gambhir SS. Molecular imaging in living subjects: seeing fundamental biological processes in a new light. Genes Dev 2003;17:545 – 80.

4. Seddon BM, Workman P. The role of functional and molecular imaging in cancer drug discovery and development. Br J Radiol 2003;76 Spec No 2:S128 – 38.

5. Wang J, Maurer L. Positron emission tomography: applications in drug discovery and drug development. Curr Top Med Chem 2005;5:1053 – 75.

6. Czernin J, Weber WA, Herschman HR. Molecular imaging in the development of cancer therapeutics. Annu Rev Med 2006;57:99 – 118.

7. Bergers G, Benjamin LE. Tumorigenesis and the angiogenic switch. Nat Rev Cancer 2003;3:401 – 10.

8. Ferrara N. VEGF and the quest for tumour angiogenesis factors. Nat Rev Cancer 2002;2:795 – 803.

9. Brooks PC, Stromblad S, Sanders LC, et al. Localization of matrix metalloproteinase MMP-2 to the surface of invasive cells by interaction with integrin $\alpha_v\beta_3$. Cell 1996;85:683 – 93.

10. De S, Razorenova O, McCabe NP, O'Toole T, Qin J, Byzova TV. VEGF-integrin interplay controls tumor growth and vascularization. Proc Natl Acad Sci U S A 2005;102:7589 – 94.

11. Ferrara N. The role of VEGF in the regulation of physiological and pathological angiogenesis. EXS 2005;209 – 31.

12. Hicklin DJ, Ellis LM. Role of the vascular endothelial growth factor pathway in tumor growth and angiogenesis. J Clin Oncol 2005;23:1011 – 27.

13. Ferrara N. Vascular endothelial growth factor: basic science and clinical progress. Endocr Rev 2004;25:581 – 611.

14. Sun J, Wang DA, Jain RK, et al. Inhibiting angiogenesis and tumorigenesis by a synthetic molecule that blocks binding of both VEGF and PDGF to their receptors. Oncogene 2005;24:4701 – 9.

15. Prewett M, Huber J, Li Y, et al. Antivascular endothelial growth factor receptor (fetal liver kinase 1) monoclonal antibody inhibits tumor angiogenesis and growth of several mouse and human tumors. Cancer Res 1999;59:5209 – 18.

16. Wedge SR, Ogilvie DJ, Dukes M, et al. ZD4190: an orally active inhibitor of vascular endothelial growth factor signaling with broad-spectrum antitumor efficacy. Cancer Res 2000;60:970 – 5.

17. Middleton G, Lapka DV. Bevacizumab (Avastin). Clin J Oncol Nurs 2004;8:666 – 9.

18. Lu E, Wagner WR, Schellenberger U, et al. Targeted *in vivo* labeling of receptors for vascular endothelial growth factor: approach to identification of ischemic tissue. Circulation 2003;108:97 – 103.

19. Blankenberg FG, Mandl S, Cao YA, et al. Tumor imaging using a standardized radiolabeled adapter protein docked to vascular endothelial growth factor. J Nucl Med 2004;45:1373 – 80.

20. Blankenberg FG, Backer MV, Levashova Z, Patel V, Backer JM. *In vivo* tumor angiogenesis imaging with site-specific labeled ^{99m}Tc-HYNIC-VEGF. Eur J Nucl Med Mol Imaging 2006;33:841 – 8.

21. Cornelissen B, Oltenfreiter R, Kersemans V, et al. *In vitro* and *in vivo* evaluation of [^{123}I]-VEGF$_{165}$ as a potential tumor marker. Nucl Med Biol 2005;32:431 – 6.

22. Li S, Peck-Radosavljevic M, Kienast O, et al. Iodine-123-vascular endothelial growth factor-165 (^{123}I-VEGF$_{165}$). Biodistribution, safety and radiation dosimetry in patients with pancreatic carcinoma. Q J Nucl Med Mol Imaging 2004;48:198 – 206.

23. Chan C, Sandhu J, Guha A, et al. A human transferrin-vascular endothelial growth factor (hnTf-VEGF) fusion protein containing an integrated binding site for ^{111}In for imaging tumor angiogenesis. J Nucl Med 2005;46:1745 – 52.

24. Collingridge DR, Carroll VA, Glaser M, et al. The development of [^{124}I]iodinated-VG76e: a novel tracer for imaging vascular endothelial growth factor *in vivo* using positron emission tomography. Cancer Res 2002;62:5912 – 9.

25. Jayson GC, Zweit J, Jackson A, et al. Molecular imaging and biological evaluation of HuMV833 anti-VEGF antibody: implications for trial design of antiangiogenic antibodies. J Natl Cancer Inst 2002;94:1484 – 93.

26. Cai W, Chen K, Mohamedali KA, et al. Positron emission tomography imaging of vascular endothelial growth factor receptor expression. J Nucl Med. In press 2006.

27. Goncalves M, Estieu-Gionnet K, Berthelot T, et al. Design, synthesis, and evaluation of original carriers for targeting vascular endothelial growth factor receptor interactions. Pharm Res 2005;22:1411 – 21.

28. Wang Y, Iyer M, Annala A, Wu L, Carey M, Gambhir SS. Noninvasive indirect imaging of vascular endothelial growth factor gene expression using bioluminescence imaging in living transgenic mice. Physiol Genomics 2006;24:173 – 80.

29. Ruoslahti E. RGD and other recognition sequences for integrins. Annu Rev Cell Dev Biol 1996;12:697 – 715.

30. Hood JD, Cheresh DA. Role of integrins in cell invasion and migration. Nat Rev Cancer 2002;2:91 – 100.

31. Xiong JP, Stehle T, Zhang R, et al. Crystal structure of the extracellular segment of integrin $\alpha_v\beta_3$ in complex with an Arg-Gly-Asp ligand. Science 2002;296:151 – 5.

32. Cai W, Chen X. Anti-angiogenic cancer therapy based on integrin $\alpha_v\beta_3$ antagonism. Anti-Cancer Agents Med Chem 2006;6:407 – 28.

33. Xiong JP, Stehle T, Diefenbach B, et al. Crystal structure of the extracellular segment of integrin $\alpha_v\beta_3$. Science 2001;294:339 – 45.

34. Cai W, Gambhir SS, Chen X. Multimodality tumor imaging targeting integrin $\alpha_v\beta_3$. Biotechniques 2005;39:S6 – 17.

35. Sipkins DA, Cheresh DA, Kazemi MR, Nevin LM, Bednarski MD, Li KC. Detection of tumor angiogenesis *in vivo* by $\alpha_v\beta_3$-targeted magnetic resonance imaging. Nat Med 1998;4:623 – 6.

36. Anderson SA, Rader RK, Westlin WF, et al. Magnetic resonance contrast enhancement of neovasculature with $\alpha_v\beta_3$-targeted nanoparticles. Magn Reson Med 2000;44:433 – 9.

37. Winter PM, Caruthers SD, Kassner A, et al. Molecular imaging of angiogenesis in nascent Vx-2 rabbit tumors using a novel $\alpha_v\beta_3$-targeted nanoparticle and 1.5 tesla magnetic resonance imaging. Cancer Res 2003;63:5838 – 43.

38. Ellegala DB, Leong-Poi H, Carpenter JE, et al. Imaging tumor angiogenesis with contrast ultrasound and microbubbles targeted to $\alpha_v\beta_3$. Circulation 2003;108:336 – 41.

39. Shohet RV, Chen S, Zhou YT, et al. Echocardiographic destruction of albumin microbubbles directs gene delivery to the myocardium. Circulation 2000;101:2554 – 6.

40. Frangioni JV. *In vivo* near-infrared fluorescence imaging. Curr Opin Chem Biol 2003;7:626 – 34.

41. Chen X, Conti PS, Moats RA. *In vivo* near-infrared fluorescence imaging of integrin $\alpha_v\beta_3$ in brain tumor xenografts. Cancer Res 2004;64:8009 – 14.

42. Cai W, Shin DW, Chen K, et al. Peptide-labeled near-infrared quantum dots for imaging tumor vasculature in living subjects. Nano Lett 2006;6: 669 – 76.

43. Achilefu S, Bloch S, Markiewicz MA, et al. Synergistic effects of light-emitting probes and peptides for targeting and monitoring integrin expression. Proc Natl Acad Sci U S A 2005;102:7976 – 81.

44. Ye Y, Bloch S, Xu B, Achilefu S. Design, synthesis, and evaluation of near infrared fluorescent multimeric RGD peptides for targeting tumors. J Med Chem 2006;49:2268 – 75.

45. Janssen ML, Oyen WJ, Dijkgraaf I, et al. Tumor targeting with radiolabeled $\alpha_v\beta_3$ integrin binding peptides in a nude mouse model. Cancer Res 2002;62:6146 – 51.

46. Sadeghi MM, Krassilnikova S, Zhang J, et al. Detection of injury-induced vascular remodeling by targeting activated $\alpha_v\beta_3$ integrin *in vivo*. Circulation 2004;110:84 – 90.

47. Line BR, Mitra A, Nan A, Ghandehari H. Targeting tumor angiogenesis: comparison of peptide and polymer-peptide conjugates. J Nucl Med 2005;46:1552 – 60.

48. Haubner R, Wester HJ, Reuning U, et al. Radiolabeled $\alpha_v\beta_3$ integrin antagonists: a new class of tracers for tumor targeting. J Nucl Med 1999; 40:1061 – 71.

49. Haubner R, Wester H-J, Weber WA, et al. Noninvasive imaging of $\alpha_v\beta_3$ integrin expression using ^{18}F-labeled RGD-containing glycopeptide and positron emission tomography. Cancer Res 2001;61:1781 – 5.

50. Haubner R, Weber WA, Beer AJ, et al. Noninvasive visualization of the activated $\alpha_v\beta_3$ integrin in cancer patients by positron emission tomography and [^{18}F]galacto-RGD. PLoS Med 2005;2:e70.

51. Chen X, Park R, Hou Y, et al. MicroPET imaging of brain tumor angiogenesis with ^{18}F-labeled PEGylated RGD peptide. Eur J Nucl Med Mol Imaging 2004;31:1081 – 9.

52. Chen X, Park R, Shahinian AH, et al. ^{18}F-labeled RGD peptide: initial evaluation for imaging brain tumor angiogenesis. Nucl Med Biol 2004;31: 179 – 89.

53. Chen X, Park R, Tohme M, Shahinian AH, Bading JR, Conti PS. MicroPET and autoradiographic imaging of breast cancer α_v-integrin expression using ^{18}F- and ^{64}Cu-labeled RGD peptide. Bioconjug Chem 2004;15:41 – 9.

54. Chen X, Tohme M, Park R, Hou Y, Bading JR, Conti PS. Micro-PET imaging of $\alpha_v\beta_3$-integrin expression with ^{18}F-labeled dimeric RGD peptide. Mol Imaging 2004;3:96 – 104.

55. Zhang X, Xiong Z, Wu X, et al. Quantitative PET imaging of tumor integrin $\alpha_v\beta_3$ expression with ^{18}F-FRGD2. J Nucl Med 2006;47:113 – 21.

56. Cai W, Zhang X, Wu Y, Chen X. A thiol-reactive ^{18}F-labeling agent, *N*-[2-(4 – 18F-fluorobenzamido)ethyl]maleimide (^{18}F-FBEM), and the synthesis of RGD peptide-based tracer for PET imaging of $\alpha_v\beta_3$ integrin expression. J Nucl Med 2006;47:1172 – 80.

57. Chen X, Hou Y, Tohme M, et al. Pegylated Arg-Gly-Asp peptide: ^{64}Cu labeling and PET imaging of brain tumor $\alpha_v\beta_3$-integrin expression. J Nucl Med 2004;45:1776 – 83.

58. Chen X, Liu S, Hou Y, et al. MicroPET imaging of breast cancer α_v-integrin expression with ^{64}Cu-labeled dimeric RGD peptides. Mol Imaging Biol 2004;6:350 – 9.

59. Chen X, Sievers E, Hou Y, et al. Integrin $\alpha_v\beta_3$-targeted imaging of lung cancer. Neoplasia 2005;7:271 – 9.

60. Wu Y, Zhang X, Xiong Z, et al. MicroPET imaging of glioma α_v-integrin expression using ^{64}Cu-labeled tetrameric RGD eptide. J Nucl Med 2005; 46:1707 – 18.

61. Cai W, Wu Y, Chen K, Cao Q, Tice DA, Chen X. *In vitro* and *in vivo* characterization of ^{64}Cu-labeled Abegrin™, a humanized monoclonal antibody against integrin $\alpha_v\beta_3$. Cancer Res 2006;66:9673 – 81.

62. Haubner R. $\alpha_v\beta_3$-integrin imaging: a new approach to characterise angiogenesis? Eur J Nucl Med Mol Imaging 2006;33 Suppl 13:54 – 63.

63. Egeblad M, Werb Z. New functions for the matrix metalloproteinases in cancer progression. Nat Rev Cancer 2002;2:161 – 74.

64. Overall CM, Lopez-Otin C. Strategies for MMP inhibition in cancer: innovations for the post-trial era. Nat Rev Cancer 2002;2:657 – 72.

65. Breyholz HJ, Schafers M, Wagner S, et al. C-5-disubstituted barbiturates as potential molecular probes for noninvasive matrix metalloproteinase imaging. J Med Chem 2005;48:3400 – 9.

66. Furumoto S, Takashima K, Kubota K, Ido T, Iwata R, Fukuda H. Tumor detection using ^{18}F-labeled matrix metalloproteinase-2 inhibitor. Nucl Med Biol 2003;30:119 – 25.

67. Giersing BK, Rae MT, CarballidoBrea M, Williamson RA, Blower PJ. Synthesis and characterization of ^{111}In-DTPA-N-TIMP-2: a radiopharmaceutical for imaging matrix metalloproteinase expression. Bioconjug Chem 2001;12:964 – 71.

68. Kopka K, Breyholz HJ, Wagner S, et al. Synthesis and preliminary biological evaluation of new radioiodinated MMP inhibitors for imaging MMP activity *in vivo*. Nucl Med Biol 2004;31:257 – 67.

69. Medina OP, Kairemo K, Valtanen H, et al. Radionuclide imaging of tumor xenografts in mice using a gelatinase-targeting peptide. Anticancer Res 2005;25:33 – 42.

70. Oltenfreiter R, Staelens L, Lejeune A, et al. New radioiodinated carboxylic and hydroxamic matrix metalloproteinase inhibitor tracers as potential tumor imaging agents. Nucl Med Biol 2004;31:459 – 68.

71. Sprague JE, Li WP, Liang K, Achilefu S, Anderson CJ. *In vitro* and *in vivo* investigation of matrix metalloproteinase expression in metastatic tumor models. Nucl Med Biol 2006;33:227 – 37.

72. Zheng QH, Fei X, Liu X, et al. Synthesis and preliminary biological evaluation of MMP inhibitor radiotracers [^{11}C]methyl-halo-CGS 27023A analogs, new potential PET breast cancer imaging agents. Nucl Med Biol 2002;29:761 – 70.

73. Bremer C, Bredow S, Mahmood U, Weissleder R, Tung CH. Optical imaging of matrix metalloproteinase-2 activity in tumors: feasibility study in a mouse model. Radiology 2001;221:523 – 9.

74. Bremer C, Tung CH, Weissleder R. *In vivo* molecular target assessment of matrix metalloproteinase inhibition. Nat Med 2001;7:743 – 8.

75. Chen J, Tung CH, Allport JR, Chen S, Weissleder R, Huang PL. Near-infrared fluorescent imaging of matrix metalloproteinase activity after myocardial infarction. Circulation 2005;111:1800 – 5.

76. Jiang T, Olson ES, Nguyen QT, Roy M, Jennings PA, Tsien RY. Tumor imaging by means of proteolytic activation of cell-penetrating peptides. Proc Natl Acad Sci U S A 2004;101:17867 – 72.

77. Zhang Y, So MK, Rao J. Protease-modulated cellular uptake of quantum dots. Nano Lett 2006:6:1988 – 92.

78. McIntyre JO, Fingleton B, Wells KS, et al. Development of a novel fluorogenic proteolytic beacon for *in vivo* detection and imaging of tumour-associated matrix metalloproteinase-7 activity. Biochem J 2004; 377:617 – 28.

79. Fonsatti E, Altomonte M, Nicotra MR, Natali PG, Maio M. Endoglin (CD105): a powerful therapeutic target on tumor-associated angiogenetic blood vessels. Oncogene 2003;22:6557 – 63.

80. Korpanty G, Grayburn PA, Shohet RV, Brekken RA. Targeting vascular endothelium with avidin microbubbles. Ultrasound Med Biol 2005;31:1279 – 83.

81. Fonsatti E, Jekunen AP, Kairemo KJ, et al. Endoglin is a suitable target for efficient imaging of solid tumors: *in vivo* evidence in a canine mammary carcinoma model. Clin Cancer Res 2000;6:2037 – 43.

82. Bredow S, Lewin M, Hofmann B, Marecos E, Weissleder R. Imaging of tumour neovasculature by targeting the TGF-β binding receptor endoglin. Eur J Cancer 2000;36:675 – 81.

83. Laferriere J, Houle F, Huot J. Regulation of the metastatic process by E-selectin and stress-activated protein kinase-2/p38. Ann N Y Acad Sci 2002;973:562 – 72.

84. Funovics M, Montet X, Reynolds F, Weissleder R, Josephson L. Nanoparticles for the optical imaging of tumor E-selectin. Neoplasia 2005; 7:904 – 11.

85. Citrin D, Scott T, Sproull M, Menard C, Tofilon PJ, Camphausen K. *In vivo* tumor imaging using a near-infrared-labeled endostatin molecule. Int J Radiat Oncol Biol Phys 2004;58:536 – 41.

86. Yang DJ, Kim KD, Schechter NR, et al. Assessment of antiangiogenic effect using ^{99m}Tc-EC-endostatin. Cancer Biother Radiopharm 2002;17: 233 – 45.